Hindawi
Advances in Civil Engineering
Volume 2019, Article ID 1312746, 16 pages
https://doi.org/10.1155/2019/1312746

Research Article

Variation in the Permeability of Intact and Fractured Rocks due to Transient Disturbances in Axial Stress or Pore Pressure

Sophea Boeut,[1] **Teppei Oshima**,[2] **Yoshiaki Fujii**,[1] **Jun-ichi Kodama**,[1] **Daisuke Fukuda**,[1] **Hiroyuki Matsumoto**,[3] **Kazumi Uchida**,[3] **and Anjula B. N. Dassanayake**[4]

[1]*Rock Mechanics Laboratory, Graduate School of Engineering, Hokkaido University, Kita 13 Nishi 8, Kita-ku, Sapporo, Hokkaido 060-8628, Japan*
[2]*DOWA Metals & Mining Co., Ltd, Tokyo, Japan*
[3]*Kushiro Coal Mine, Kushiro, Japan*
[4]*University of Moratuwa, Moratuwa, Sri Lanka*

Correspondence should be addressed to Sophea Boeut; boeurtsophea@gmail.com

Received 8 February 2019; Accepted 21 May 2019; Published 13 June 2019

Academic Editor: Sanjay Nimbalkar

A persistent increase in the permeability of rock mass caused by transient stress disturbances, if present, could explain the variation in the groundwater level in far fields, increase in petroleum production caused by earthquakes or artificial vibrations in enhanced oil recovery, and induction of earthquakes by seismic waves in intermediate and far fields. However, it has not been verified whether the transient stress disturbances induce an increase or decrease in the rock permeability. In this study, the permeability values of intact and triaxially fractured Kushiro Cretaceous sandstone and Shikotsu welded tuff were measured before and after transient axial stress or pore pressure disturbances to clarify the effects of transient stress disturbances on rock permeability. According to the experimental results, the stress disturbances showed either decreasing or increasing effects on the permeability depending on the rock type and experimental conditions. However, when focusing on the fractured rocks rather than the intact ones, which would be more important in field applications, the argillaceous Kushiro Cretaceous sandstone mainly exhibited decreasing effects and the glassy Shikotsu welded tuff mainly exhibited increasing effects.

1. Introduction

Large earthquakes can lead to persistent variation in the groundwater level in near fields (within fault length) [1, 2]. This is observed because of the persistent variation in the permeability of rock mass, which is due to the variation in strain; this variation is in turn caused by fault movement. Such variations may also occur in an intermediate field (from one to multiple fault lengths) [3]. However, it was shown that those persistent modifications in the groundwater level may even occur in the far field (many fault lengths), up to thousands of kilometers from the epicenter [4, 5].

The persistent variation in the groundwater level in the far field cannot be explained by the variation in permeability associated with the strain alteration due to the fault movement; this is because the variation in strain in the far field is transient. Manga et al. [4] suggested that the persistent variation in the groundwater level might rather be due to a persistent increase in rock mass permeability, which is in turn caused by transient stress disturbances from the seismic waves of earthquakes.

A persistent increase in the permeability of rock mass caused by transient stress disturbances, if present, could explain the increase in petroleum production caused by earthquakes or artificial vibrations [6] as that seen in enhanced oil recovery [7]. Manga et al. [4] also implied the possibility that seismic waves induce earthquakes in the intermediate and far fields. Even the decrease in giant ($M \geq 8$) earthquakes in the 1960s and 1990s, during which time the United States, the Union of Soviet Socialist Republics, and other countries frequently carried out underground nuclear explosion tests [8], might be explained by the induction of

numerous small earthquakes. These earthquakes were a result of the variation in rock mass permeability due to transient stress disturbances, which were in turn caused by the seismic waves of the test explosions.

However, it has not been verified whether the transient stress disturbances induce an increase or decrease in the rock permeability (Table 1). In this study, the permeability values of intact and triaxially fractured Kushiro Cretaceous sandstone and Shikotsu welded tuff were measured before and after transient axial stress or pore pressure disturbances to clarify the effects of transient stress disturbances on rock permeability.

It is difficult to compare the results from previous studies (Table 1) because the rock types were different from study to study, the permeability was measured for only one rock condition (intact, fractured, or in situ), and for only one type of disturbance (pore pressure, axial displacement, or axial stress) in each study. In this research, the permeability values of both the intact and fractured rock specimens were measured, and the disturbance types included both transient axial stress and pore pressure so that the effects of transient stress disturbances on the permeability between rock types, rock conditions, and disturbance types could be compared.

2. Materials and Methods

2.1. Rock Samples. The Kushiro Cretaceous sandstone was sampled from the Cretaceous sandstone layer of the Kushiro Coal Mine [13], which is located in the eastern region of Hokkaido, Japan. Methane gas has been extracted from the Cretaceous layer underlying the Paleogene coal-bearing formation.

The rock comprises of a matrix of quartz, plagioclases, and silt-size smectite (Figure 1, Table 2) and is classified as wacke fine-grained sandstone. The grain sizes of the quartz are between 0.2 and 0.4 mm, and the plagioclase grains are less than 0.2 mm and have an angular to subangular form. The average porosity is 11% (Table 3).

A rock block of Shikotsu welded tuff having a porosity of 32% (Table 3) was taken from Sapporo, Japan. The glassy rock sample, which originated from pyroclastic deposits from the eruption of the Shikotsu volcano 40,000 years ago, is predominantly composed of plagioclase, hypersthene, augite, hornblende, and transparent volcanic glass having a felt-like structure in the matrix. The mineral grain sizes are between 0.3 and 1.5 mm for the plagioclase, approximately 0.5 mm for the hypersthene, 0.3–0.7 mm for the augite, and 0.5–1.0 mm for the hornblende [14].

2.2. Sample Preparation and Permeability Measurement. Cylindrical specimens (30 mm in diameter, 60 mm in height) were bored from the 65 mm diameter Kushiro Cretaceous sandstone cores along the vertical drilling axis and from the rock block of the Shikotsu welded tuff along the slowest (1.67 km/s) P-wave velocity direction. The velocities in the two other perpendicular directions were 1.82 km/s and 2.11 km/s. The specimens were dried at 80°C in an oven for approximately two days before being vacuum-saturated in pure water for 3 days. Each specimen was connected to a pair of stainless-steel end pieces that had a center hole to allow water to flow through the specimen. A coating of silicon sealant was applied to the lateral surface of each specimen to maintain the water flow within the specimens. A heat-shrinkable tube was used to jacket the specimen with the end pieces to prevent direct contact of the confining fluid with the specimen. Each jacketed specimen was vacuum-saturated again for 24 h and placed in an ultracompact triaxial cell ([15], Figure 2). Axial stress or pore pressure transient disturbances were applied to the intact specimens and then to triaxially fractured specimens.

For the Kushiro Cretaceous sandstone (Table 4), the confining pressures were 3, 10, or 15 MPa. The pore pressure was 1 MPa at the bottom of the specimen, and the upper end of the specimen was open to the atmosphere (Figure 2). The axial stress disturbances were triangular at 0.5 Hz for 200 s (Figure 3(a)), and the amplitude was up to 11 MPa. The rectangular disturbances of pore pressure fluctuated between 0.2 and 1.8 MPa. A pore pressure (P_P) of 1 MPa in the constant hydrostatic stress state was the initial pore pressure, and the minimum pore pressure ($P_{P\text{-min}}$) was first manually applied followed by the maximum pore pressure ($P_{P\text{-max}}$). The disturbances had a duration of approximately 200 s, with frequency between 0.05 and 0.18 Hz under a 10 MPa confining pressure (Table 4 and Figure 3(b)). Considering the low permeability, a $10^{-5}\,s^{-1}$ (0.036 mm/s) strain-rate-controlled triaxial compression was applied. It should be noted that the axial stress disturbances for the intact rocks might also have caused pore pressure disturbances inside the specimens because of the low permeability. On the contrary, pore pressure disturbances would not induce axial stress disturbances, even for intact specimens, because the response of the loading frame was sufficiently rapid.

For the Shikotsu welded tuff (Table 5), nearly rectangular axial stress disturbances were applied with pore pressures of 0.1 and 0.5 MPa and a confining pressure of 5 MPa (Figure 4(a)). Axial stress disturbance amplitudes of 0 or 8 MPa at 0.05 Hz for 200 s were applied (Table 5). The same pore pressure, confining pressure, and disturbance frequency were used for the rectangular transient pore pressure disturbances. The applied disturbance amplitudes were between 0 and 0.8 MPa. The triaxial compression rate was set at $10^{-4}\,s^{-1}$ (0.36 mm/s), considering the high permeability.

The axial stress disturbances would not cause pore pressure disturbances inside a specimen, even for the intact rocks, because of their high permeability.

The disturbance frequency was first set at 0.5 Hz for the axial stress disturbances on the Kushiro Cretaceous sandstone simulating a moderate earthquake. However, the frequency varied because of the limiting speed for the manual operation of the syringe pump and it was finally set at 0.05 Hz. The results would have been slightly affected by the differences in the disturbance wave shapes. Furthermore, the differences in the disturbance frequency may have quantitatively affected the results. However, the effects of this difference would not be sufficient to lead to opposite conclusions.

The permeability values of the intact rock before and after the transient stress disturbances in the prefailure

Table 1: Experimental conditions and effect of stress disturbances on permeability.

Experiments	Frequency (Hz)	Peak amplitude	Disturbances	Samples		Permeability response
Elkhoury et al. [9]	0.05	0.02–0.3 MPa	Pore pressure	Fractured in situ	Berea sandstone	Increase
Roberts [10]	25–75	0.3–1.2 MPa	Axial stress	Intact	Berea sandstone	Increase
Shmonov et al. [11]	0.05–20	Strains 10^{-4}–10^{-3}	Axial stress	Intact	Limestone basalts gabbro	Increase (high $T = 130^{\circ}$C–250°C) Decrease (low $T = 20^{\circ}$C)
Liu & Manga [12]	0.3–2.5	Strain 10^{-4}	Axial displacement	Fractured	Sandstone	Decrease

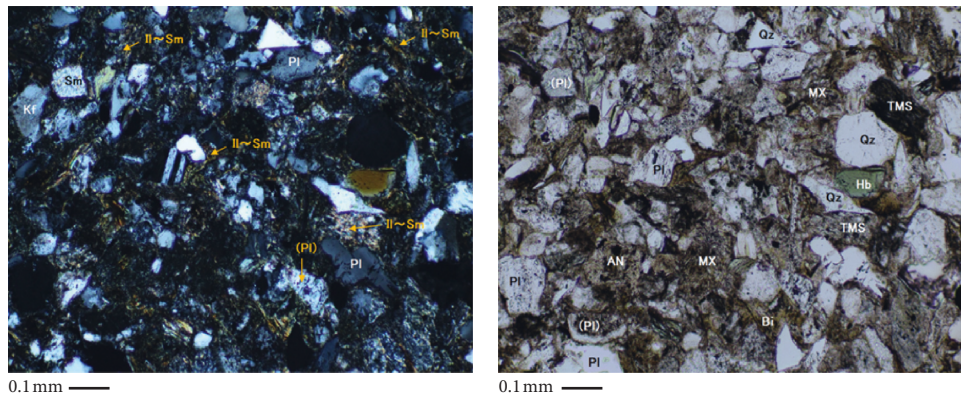

(a) (b)

Figure 1: Microscopic images of the Kushiro Cretaceous sandstone. Qz: quartz ($\phi \leq 0.2$–0.4 mm), Pl: plagioclases ($\phi \leq 0.2$ mm), Mx: matrix (Sm–Il: smectite–illite (silt-size mineral pieces)), Kf: potash feldspar ($\phi \leq 0.2$ mm), Bi: biotite ($\phi \leq 0.2$–0.5 mm), Hb: ordinary amphibole ($\phi \leq 0.15$ mm), AN: andesite ($\phi \leq 0.2$ mm), TMS: transformed mudstone ($\phi \leq 0.25$ mm), Mc: mica, and Chl: chlorite.

Table 2: Mineral composition of the Kushiro Cretaceous sandstone from XRD analysis.

Qz	Pl	Kf	Am	Hm	Mc	Chl	Sm
Very abundant	Very abundant	Abundant	Very little	Little	Little	Little	Medium

Qz: quartz; Pl: plagioclases; Kf: potash feldspar; Am: amphibole; Hm: hematite; Mc: mica; Chl: chlorite; Sm: smectite.

Table 3: Physical properties of the rock samples shown as the average value (number of specimens) ± standard deviation.

Properties	Kushiro Cretaceous sandstone		Shikotsu welded tuff	
	Dry	Saturated	Dry	Saturated
Porosity (%)	10.53 (9) ± 2.43		31.65 (18) ± 1.65	
Density (g/cm^3)	2.37 (9) ± 0.02	2.48 (9) ± 0.02	1.30 (18) ± 0.01	1.62 (18) ± 0.02
V_P (km/s)	3.35 (9) ± 0.14	3.04 (9) ± 0.16	2.14 (18) ± 0.07	1.92 (18) ± 0.14

regime, k_1 and k_2, respectively, and those of the fractured rock before and after the transient stress disturbances in the postfailure regime, k_3 and k_4, respectively, were evaluated by substituting the flow rate, which was calculated based on the variations in the water volume in the syringe pump over 24 h for the Kushiro Cretaceous sandstone (Figure 3) or over 60 s for the Shikotsu welded tuff (Figure 4). These permeability values were calculated by substituting the flow rate into the following Darcy's equation:

$$k = \frac{q\mu}{A}\left(\frac{dp}{dx}\right)^{-1}, \quad (1)$$

where k (m^2) is the permeability, q is the flow rate (m^3/s), μ is the fluid viscosity (Pa·s), A is the cross-sectional area (m^2) of the specimen, and dp/dx is the pressure gradient (Pa/m). The viscosity of water (μ) is 9.57×10^{-4} (Pa·s) at 295 K, which is the air temperature of the testing room that was kept constant with the aid of an air conditioner.

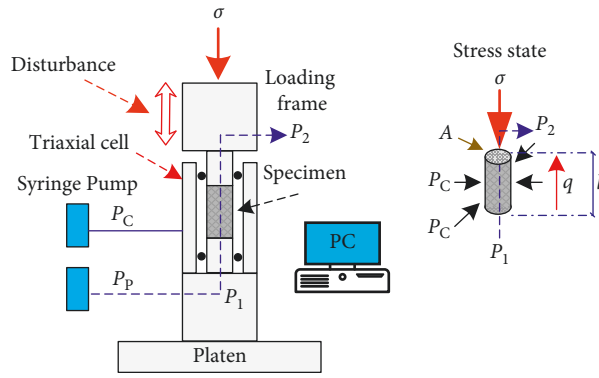

Figure 2: Permeability measurement apparatus.

Table 4: Experimental conditions for the Kushiro Cretaceous sandstone.

Axial stress disturbances							Pore pressure disturbances						
Samples	Constant hydrostatic stress		Transient axial stress				Constant hydrostatic stress			Transient pore pressure			
	P_P	P_C	σ_A	$\Delta\sigma_A$	$\sigma_{A\text{-min}}$	$\sigma_{A\text{-max}}$	Samples	P_P	P_C	ΔP_P	P_P-min	P_P-max	f
AS-KCS1	1	10	10	1	2	4	P_p-KCS1	1	10	0.2	0.9	1.1	0.15
AS-KCS2				0	10	10	P_p-KCS2			0.6	0.7	1.3	0.09
AS-KCS3				1	9.5	10.5	P_p-KCS3			0.8	0.9	1.7	0.05
AS-KCS4				3	8.5	11.5	P_p-KCS4			1	0.5	1.5	0.18
AS-KCS5				4	8	12	P_p-KCS5			1.4	0.3	1.7	0.09
AS-KCS6				5	7.5	12.5	P_p-KCS6			1.8	0.1	1.9	0.1
AS-KCS7				7	6.5	13.5	P_p-KCS7			1.8	0.1	1.9	0.1
AS-KCS8				9	5.5	14.5	P_p-KCS8			1.86	0.07	1.93	0.12
AS-KCS9				11	4.5	15.5	P_p-KCS9			1.88	0.07	1.95	0.1
AS-KCS10		15	15	1	14.5	15.5							
AS-KCS11				5	12.5	17.5							

P_C: confining pressure; P_P: pore pressure; $\Delta\sigma_A$: axial stress disturbance amplitude; ΔP_P: pore pressure disturbance amplitude; P_P-min: minimum pore pressure; P_P-max: maximum pore pressure; f: frequency. Unit of stresses is in mega Pascal (MPa) and frequency is in hertz (Hz).

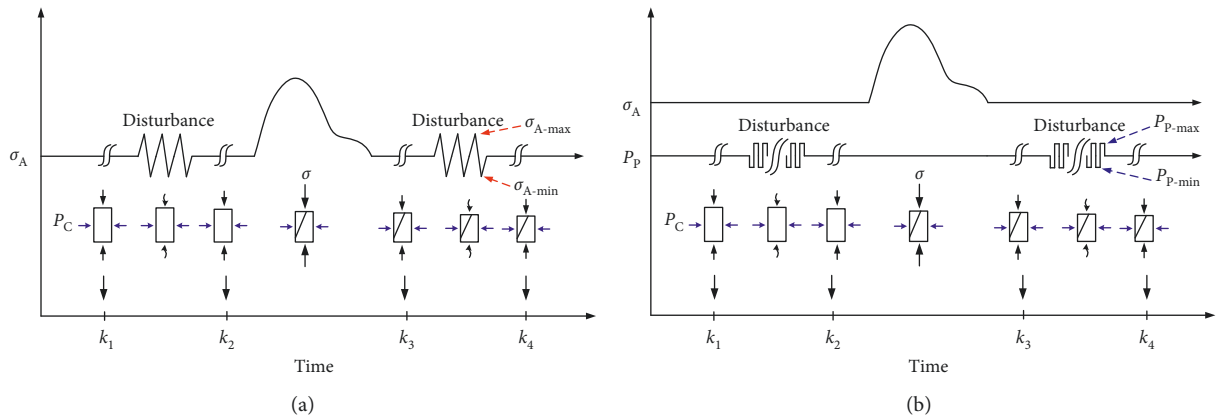

Figure 3: Experimental procedure for the Kushiro Cretaceous sandstone. (a) Axial stress disturbances; (b) pore pressure disturbances.

3. Results of the Kushiro Cretaceous Sandstone

3.1. Axial Stress Disturbances. According to the stress-strain curves, the Kushiro Cretaceous sandstone showed brittle failure in all specimens (Figure 5(a)). The maximum stress under the 10 MPa confining pressure was in the range of 90–150 MPa and slightly increased as the transient stress amplitude increased (Figure 5(b)).

The variation in permeability at the time of axial stress disturbance for some specimens in each hydrostatic stress state is presented in Figure 6, and the impacts of both transient stress disturbance and failure are shown in

Table 5: Experimental condition for the Shikotsu welded tuff.

Axial stress disturbance							Pore pressure disturbances					
Samples	Constant hydrostatic stress			Transient axial stress			Constant hydrostatic stress			Transient pore pressure		
	P_C	P_P	σ_A	$\Delta\sigma_A$	$\sigma_{A\text{-min}}$	$\sigma_{A\text{-max}}$	Samples	P_C	P_P	ΔP_P	P_P-min	P_P-max
AS-T1							P_p-T1					
AS-T2				0	5	5	P_p-T2			0	0.5	0.5
AS-T3		0.5					P_p-T3					
AS-T4							P_p-T4					
AS-T5				8	1	9	P_p-T5		0.5	0.1	0.45	0.55
AS-T6							P_p-T6					
AS-T7							P_p-T7					
AS-T8	5		5	0	5	5	P_p-T8	5		0.8	0.1	0.9
AS-T9		0.1					P_p-T9					
AS-T10				8	1	9	P_p-T10					
AS-T11							P_p-T11			0	0.1	0.1
							P_p-T12		0.1			
							P_p-T13					
							P_p-T14			0.06	0.07	0.13
							P_p-T15					

P_C: confining pressure; P_P: pore pressure; $\Delta\sigma_A$: axial stress disturbance amplitude; ΔP_P: pore pressure disturbance amplitude; P_P-min: minimum pore pressure; P_P-max: maximum pore pressure. Unit of stresses is mega Pascal (MPa).

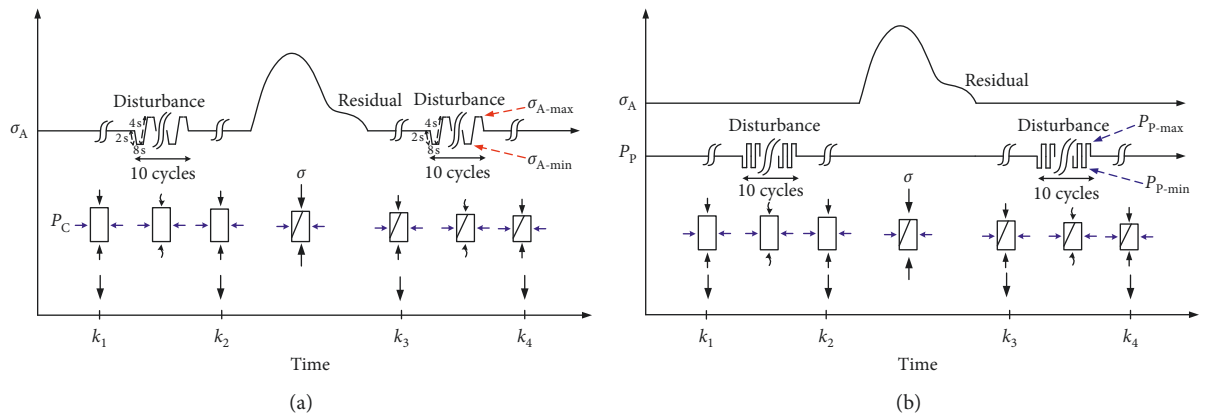

Figure 4: Experimental procedure for the Shikotsu welded tuff. (a) Axial stress disturbances; (b) pore pressure disturbances.

Figure 7. The permeability of this sandstone increased owing to the failure (observed in the variation in permeability in Hold-2 to Hold-3, Figure 6, or k_2 to k_3, Figure 7) as was reported for the Kimachi sandstone, which is a neogene tuffaceous sandstone in Japan [15]. This occurred although the axial stress disturbances caused the permeability values of the intact rocks (variation in permeability in Hold-1 to Hold-2, Figure 6, or k_1 to k_2, Figure 8(a)) and fractured rocks (variation in permeability in Hold-3 to Hold-4, Figure 6, or k_3 to k_4, Figure 9(a)) to decrease.

The permeability of the intact specimen, which is basically shown in Hold-1 and Hold-2, was reduced, even with no stress disturbances (Figure 6(a)), and the reduction was not affected by the axial stress disturbance amplitude (Figures 6 and 8(a)). However, the reduction increased as the confining pressure increased (Figure 8(b)). According to the above results, the permeability reduction of the intact rock (decrease in permeability from Hold-1 to Hold-2, or k_1 to k_2, Figure 8) could mainly be attributed to consolidation over time under the confining pressure.

The decreased effect on permeability was elucidated for fractured rocks referring to Hold-3 (pre-disturbance) and Hold-4 (post-disturbance) (Figure 6). The permeability had almost no variation under zero disturbances (Figure 6(a)); however, at the time of the disturbances, the permeability decreased (Figures 6(b)–6(d)). The reduction from k_3 to k_4 of the fractured rocks (Figure 9(a)) was small at zero stress disturbance amplitude, and it increased with the disturbance amplitude. This decrease in permeability did not depend on the confining pressure (Figure 9(b)). Therefore, the above described usual consolidation would not be a predominant mechanism. Instead, the stress disturbances may have been enhanced either by the closure of the rupture planes or by the production of fine gouge particles (Figure 10(b)), the

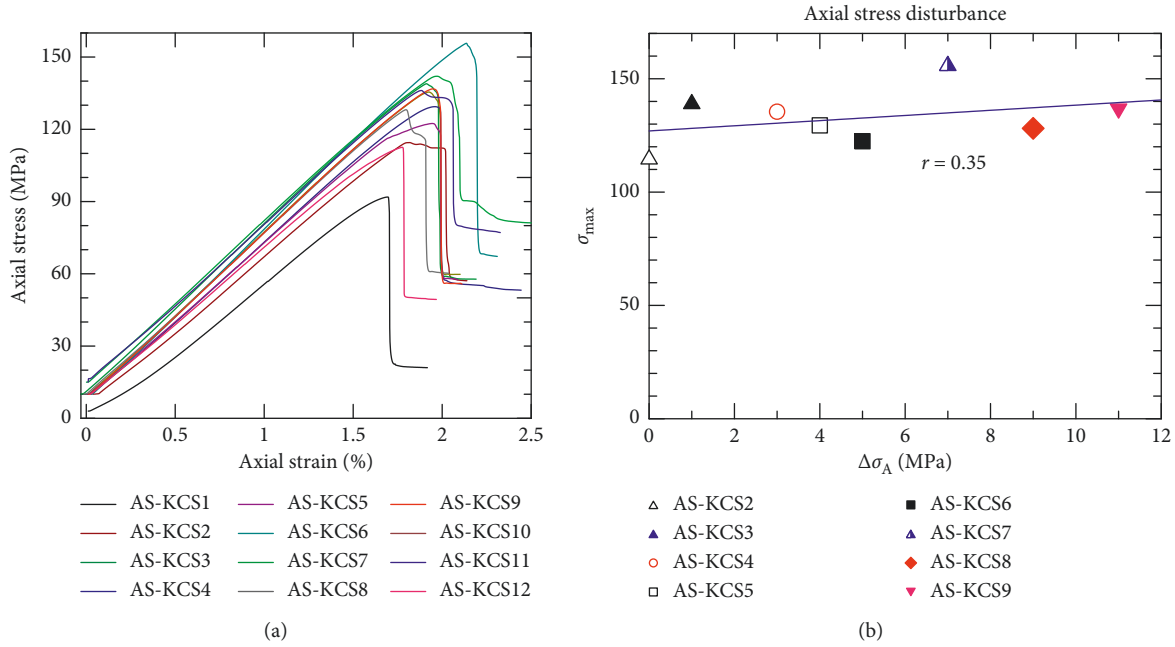

FIGURE 5: (a) Stress-strain curves and (b) maximum stress (σ_{max}) vs. the amplitudes of the axial stress disturbances ($\Delta\sigma_A$) under $P_C = 10$ MPa of the Kushiro Cretaceous sandstone.

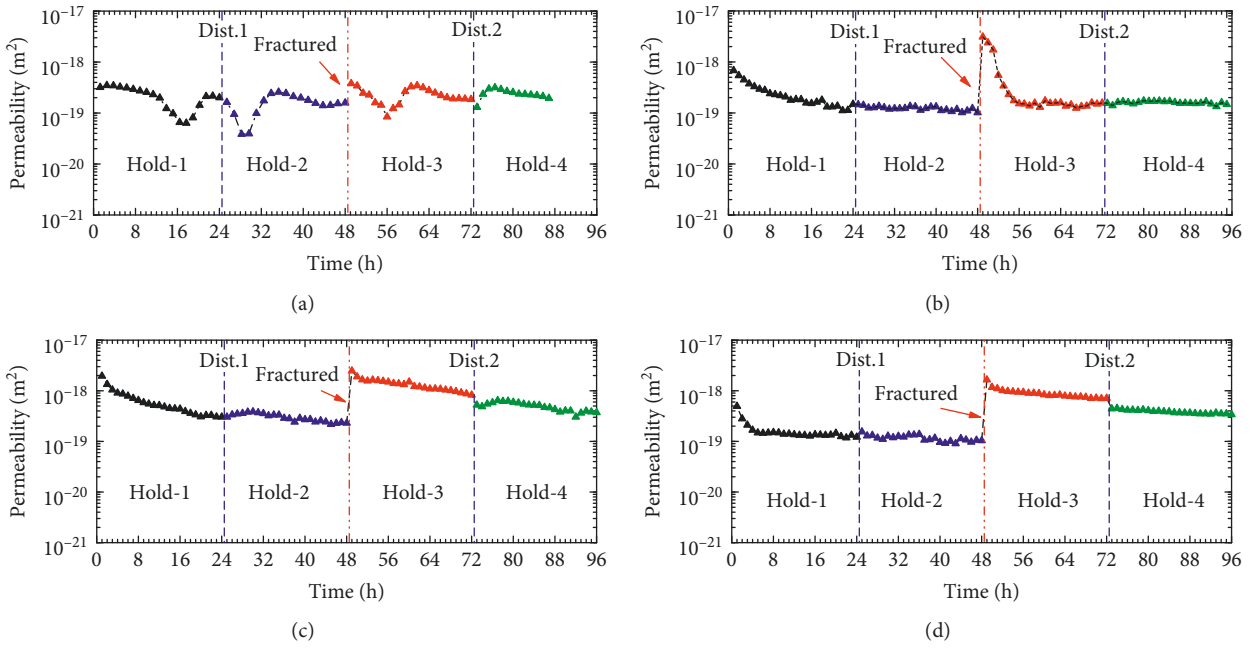

FIGURE 6: Variation in permeability in each hydrostatic stress state (Hold-1, Hold-2, Hold-3, and Hold-4) at the time of axial stress disturbance for the entire experiment: (a) AS-KCS2, (b) AS-KCS5, (c) AS-KCS8, and (d) AS-KCS9. Dist. 1 and Dist. 2 are the disturbances in prefailure and postfailure.

sizes of which varied from 10 μm to 500 μm, and they either caused clogs or settled at the points of the rupture planes that have the smallest apertures (Figure 10(c), [9, 16, 17]).

3.2. Pore Pressure Disturbances. Specimens for the pore pressure disturbance tests were prepared from another rock core obtained from a slightly different depth. All specimens failed in a brittle manner. The maximum stresses were in the range of 70–90 MPa (Figure 11(a)) and increased slightly with the pore pressure disturbance amplitude (Figure 11(b)). Permeability increased due to failure (k_2 to k_3) but decreased due to pore pressure disturbances (k_1 to k_2, and k_3 to k_4)

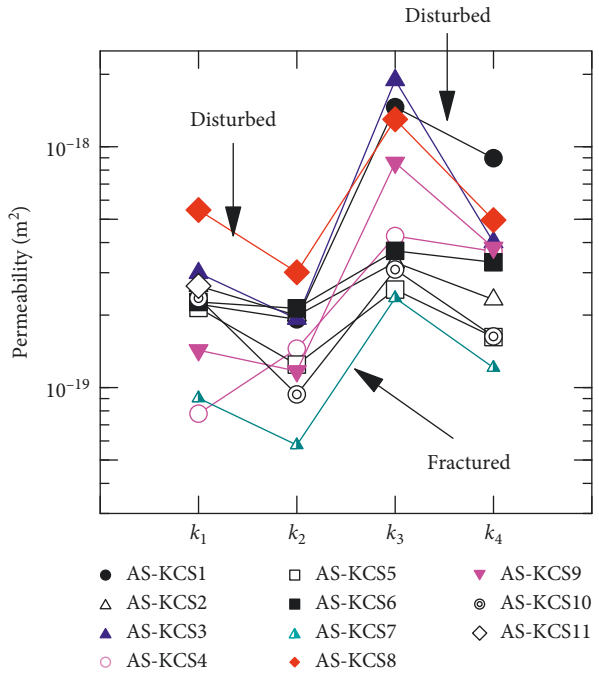

Figure 7: Variation in permeability in each hydrostatic stress state at the time of axial stress disturbances and triaxial compression.

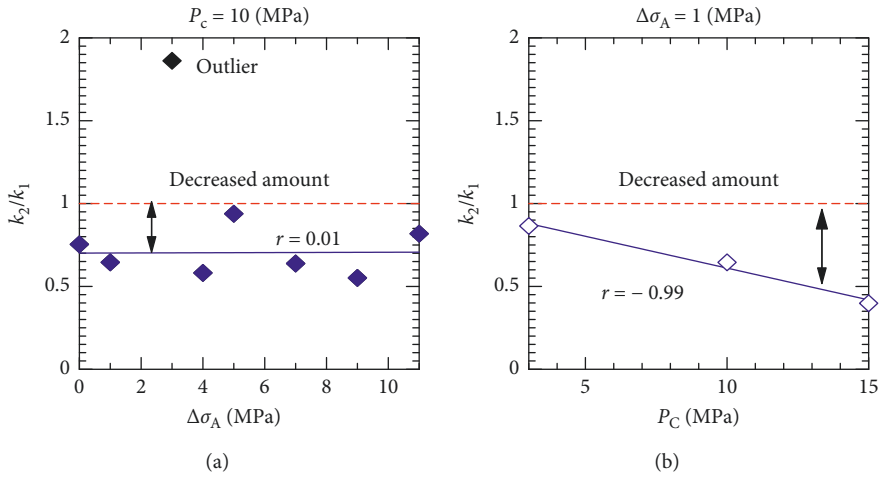

Figure 8: Permeability ratio vs. (a) axial stress disturbance amplitude and (b) confining pressure of the intact rocks. The outlier data point was ignored for the regression analysis.

(Figures 12 and 13). The y-intercept of Figure 14(a) shows the reduction in the intact rock permeability (k_1 to k_2) at zero disturbance. This would imply the effect of consolidation over time. The reduction decreased as the pore pressure disturbance amplitudes increased. Even for a specimen, k_2 was larger than k_1 under larger pore pressure disturbances (Figures 12(c) and 14(a)). This increase in the permeability could be induced by the formation of microfractures due to the pore pressure disturbances. However, as shown in Figure 6(b), the strength was not reduced with pore pressure disturbances, and hence, the formation of microfractures would not be the main mechanism. The removal of the barriers that clogged the existing pathways [4, 18, 19] would be a preferable explanation for this finding.

The reduction in permeability due to pore pressure disturbances for the fractured specimens (in postfailure, Hold-3 to Hold-4 in Figure 12, or k_3 to k_4 in Figure 14(b)) was not very large at zero disturbances and slightly increased as the pore pressure disturbance amplitude increased, although the r value (the coefficient of correlation) is low. The mechanisms would be similar to those of the fractured rocks with axial stress disturbances.

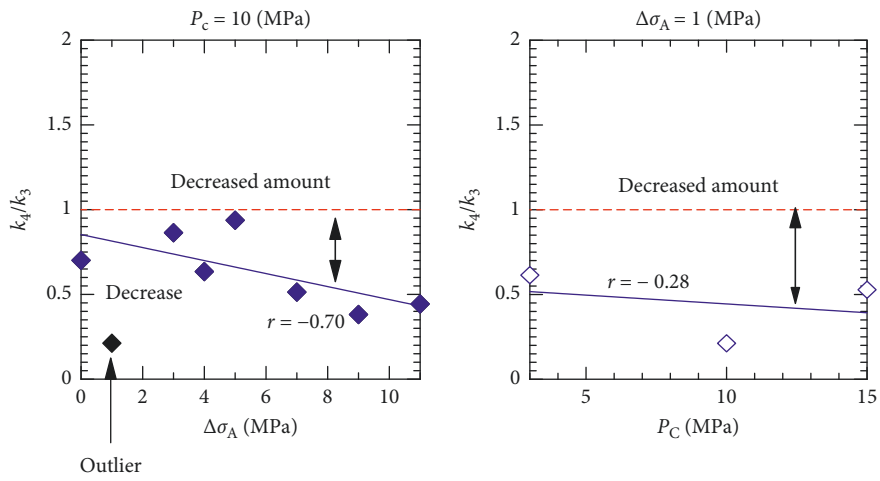

Figure 9: Permeability ratio vs. (a) axial stress disturbance amplitude and (b) confining pressure of the fractured rocks.

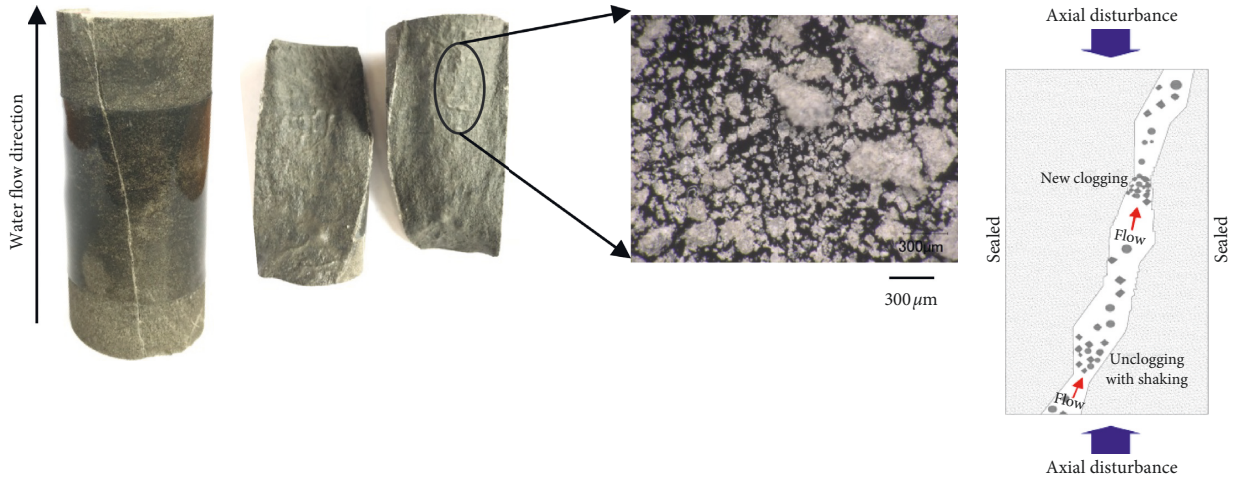

Figure 10: A specimen after an experiment (P_p-KCS3): (a) specimen showing the rupture plane, (b) gouge along the rupture plane and the microscopic image of the particles along the rupture plane, and (c) clogging and unclogging of an aperture by particles [12].

4. Result of the Shikotsu Welded Tuff

The Shikotsu welded tuff specimens failed in a ductile manner with slight stress drops (Figures 15(a) and 16(a)). The maximum stress was affected by neither the axial stress (Figure 15(b)) nor the pore pressure disturbances (Figure 16(b)).

4.1. Axial Stress Disturbances. The axial stress disturbance tests were conducted under 0.5 (Figure 17) or 0.1 MPa (Figure 18) in pore pressure. With the application of 0.5 MPa in pore pressure, the permeability showed an increase for the intact rocks (Figure 17(b)). This would occur because of the cleaning of the pore throats and the micropathways by the rapid water flow [12, 18, 19]. The increased permeability was not affected by the disturbance amplitude (Figure 17(b)). The permeability decreased from k_2 to k_3 due to rock failure (Figure 17(a)), and this result is the same as those presented by Alam et al. [15] for the same rock type. This reduction in permeability may be due to the crushing of the matrix that consists of volcanic glass (Figure 19(a)). The permeability further decreased from k_3 to k_4 at zero disturbances (Figure 17(c)). This would be due to the closure of the rupture planes and the clogging of the smallest apertures by some fine particles over time. These decreases were reduced as the disturbance amplitude increased (Figure 17(c)). This would be due to the generation and unclogging of the microfracture paths (Figure 19(b)) [4, 12, 20, 21].

Under a pore pressure of 0.1 MPa, the permeability decreased from k_1 to k_2 and k_3 (Figure 18(a)). The reduced permeability from k_1 to k_2 (Figure 18(b)) was almost constant with the axial stress disturbance amplitudes for the intact rocks. This may suggest that the rock was slightly consolidated over time and that the water flow was not sufficiently rapid to

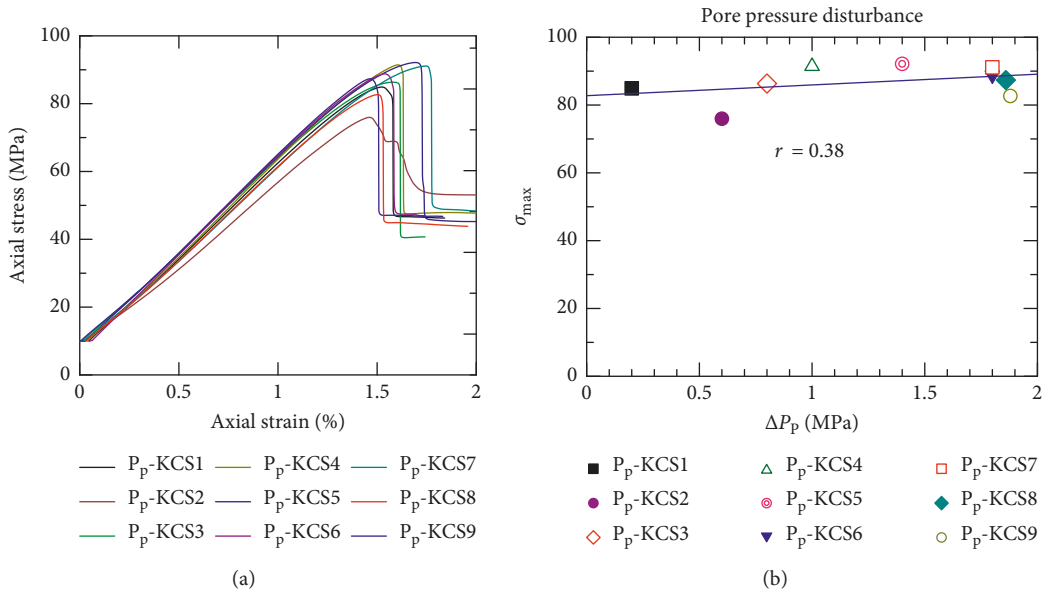

FIGURE 11: (a) Stress-strain curves and (b) maximum stress (σ_{max}) vs. amplitudes of the pore pressure disturbances (ΔP_P) of the Kushiro Cretaceous sandstone.

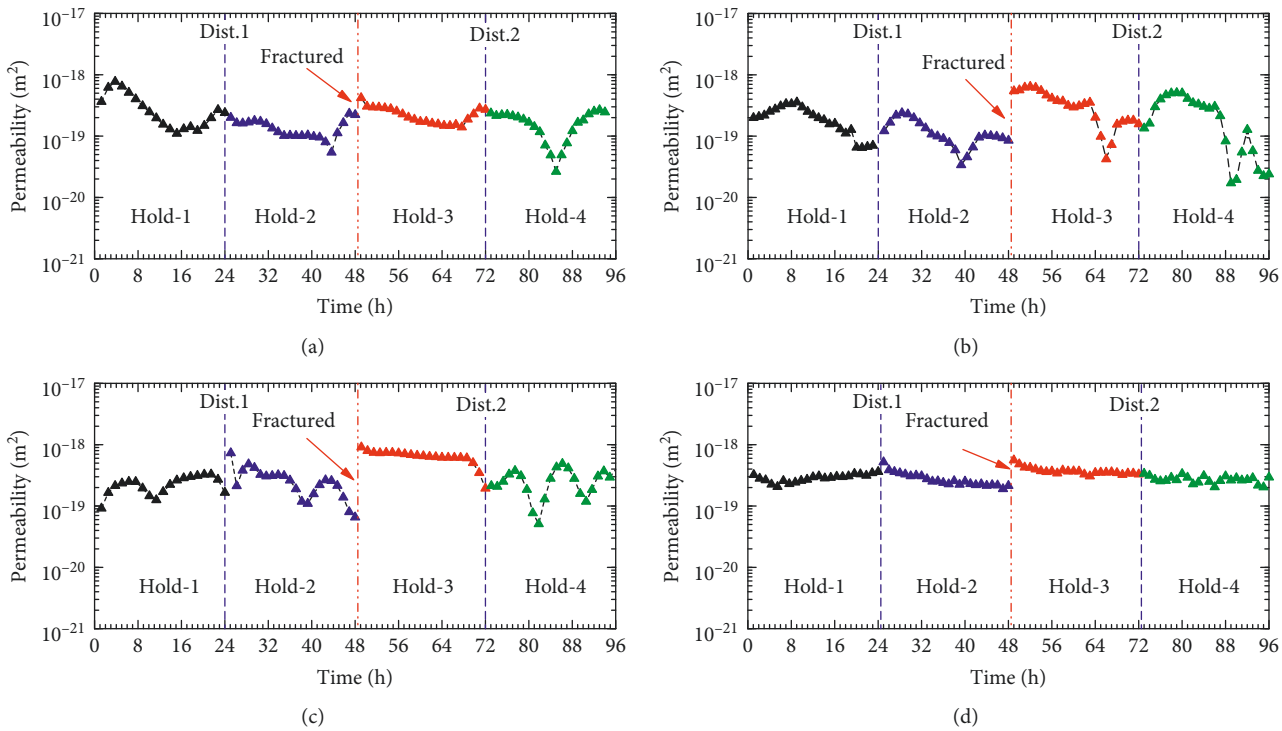

FIGURE 12: Variation in permeability in each hydrostatic stress state (Hold-1, Hold-2, Hold-3, and Hold-4) at the time of transient pore stress disturbances for the whole experiment: (a) P_p-KCS1, (b) P_p-KCS4, (c) P_p-KCS6, and (d) P_p-KCS7. Dist. 1 and Dist. 2 are the disturbances in prefailure and postfailure, respectively.

clean up the pore throats. The permeability decreased for the fractured rocks at zero stress disturbances (k_3 to k_4, Figure 18(c)). However, the reduction decreased as the stress disturbances increased (Figure 18(c)), which was probably due to mechanisms similar to those of the 0.5 MPa case (Figure 17(c)).

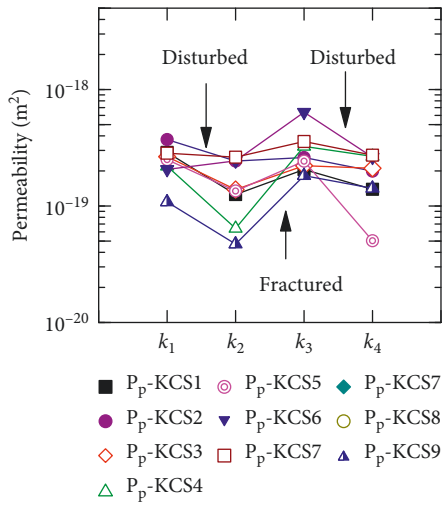

Figure 13: Permeability variation due to pore pressure disturbances and triaxial compression under $P_C = 10$ MPa.

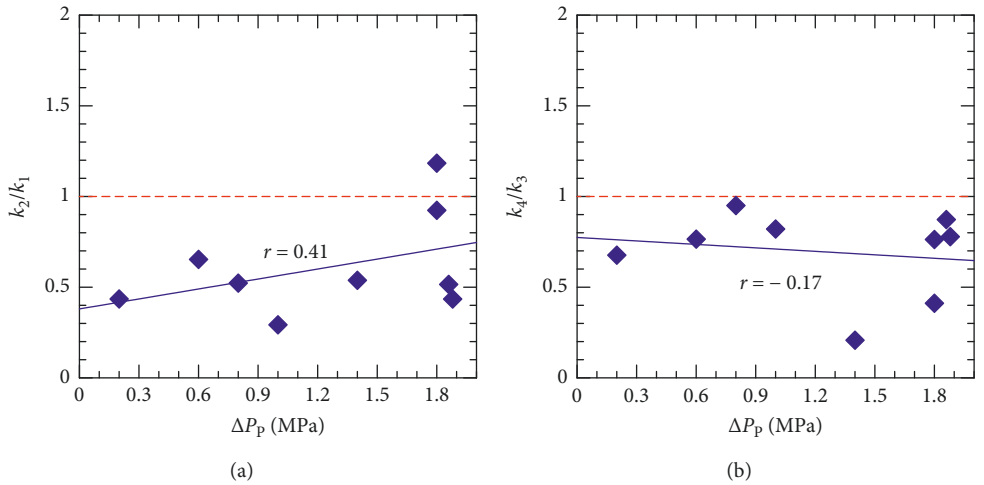

Figure 14: Effect of pore pressure disturbances on the permeability ratio of the Kushiro Cretaceous sandstone: (a) intact rocks and (b) fractured rocks.

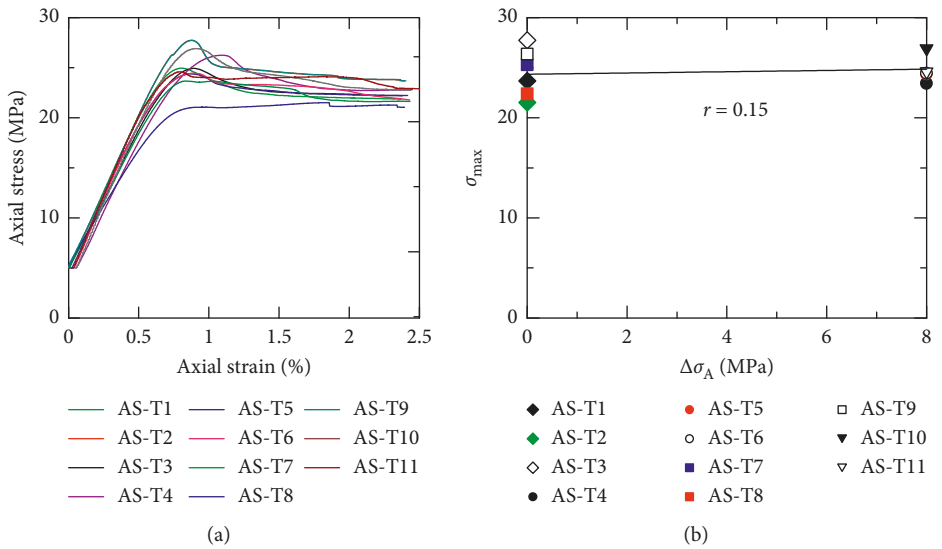

Figure 15: (a) Stress-strain curves and (b) maximum stress (σ_{max}) vs. amplitude of the axial stress disturbances ($\Delta\sigma_A$) of the Shikotsu welded tuff.

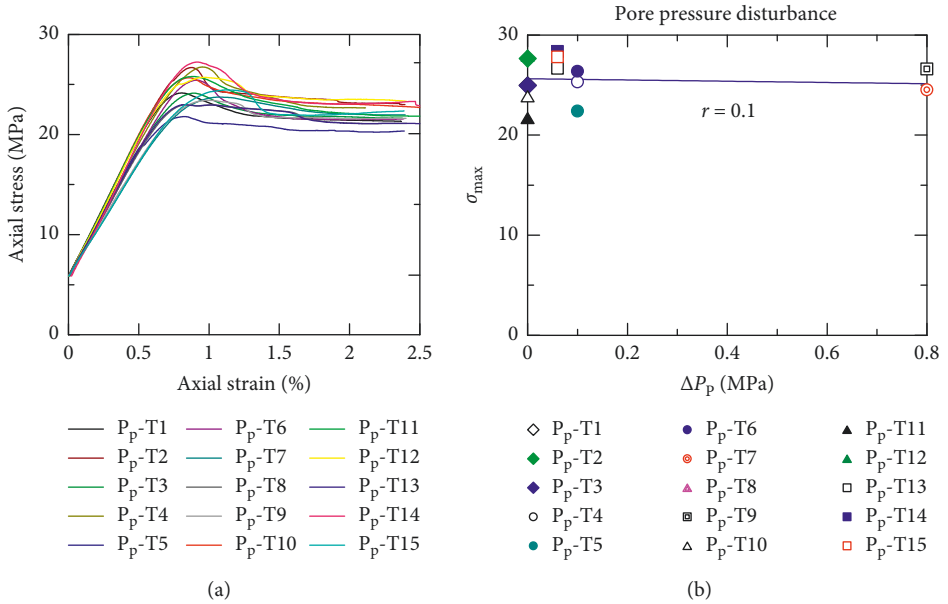

FIGURE 16: (a) Stress-strain curves and (b) maximum stress (σ_{max}) vs. the amplitude of the pore pressure disturbance (ΔP_P) of the Shikotsu welded tuff.

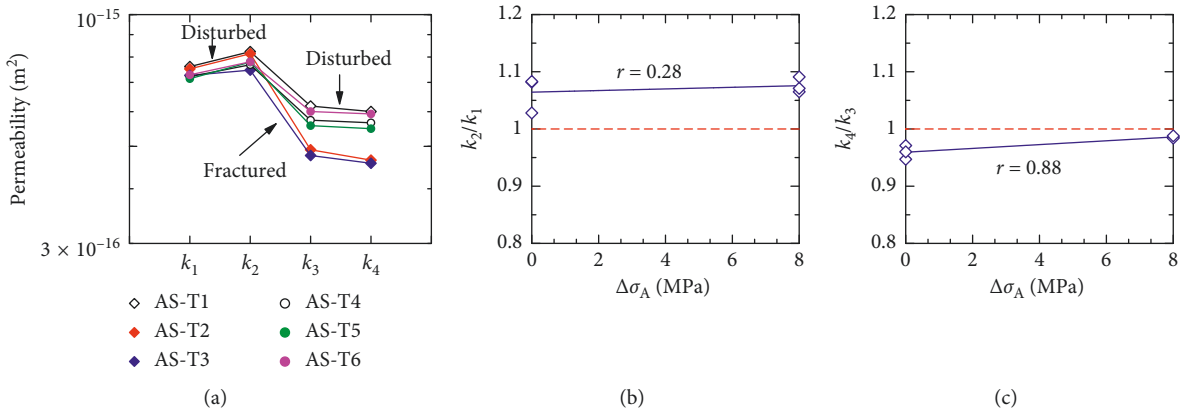

FIGURE 17: Variation in permeability (a), and permeability ratios of the intact rocks (b) and fractured rocks (c) ($P_P = 0.5$ MPa) due to transient axial stress disturbances and triaxial compression of the Shikotsu welded tuff.

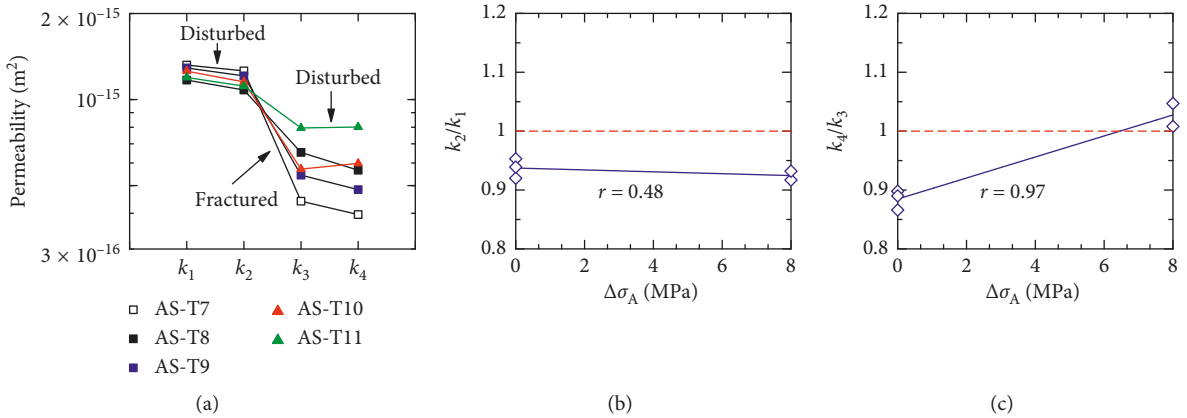

FIGURE 18: Variation in permeability (a), and permeability ratios of the intact rocks (b) and fractured rocks (c) ($P_P = 0.1$ MPa) due to transient axial stress disturbances and the triaxial compression of the Shikotsu welded tuff.

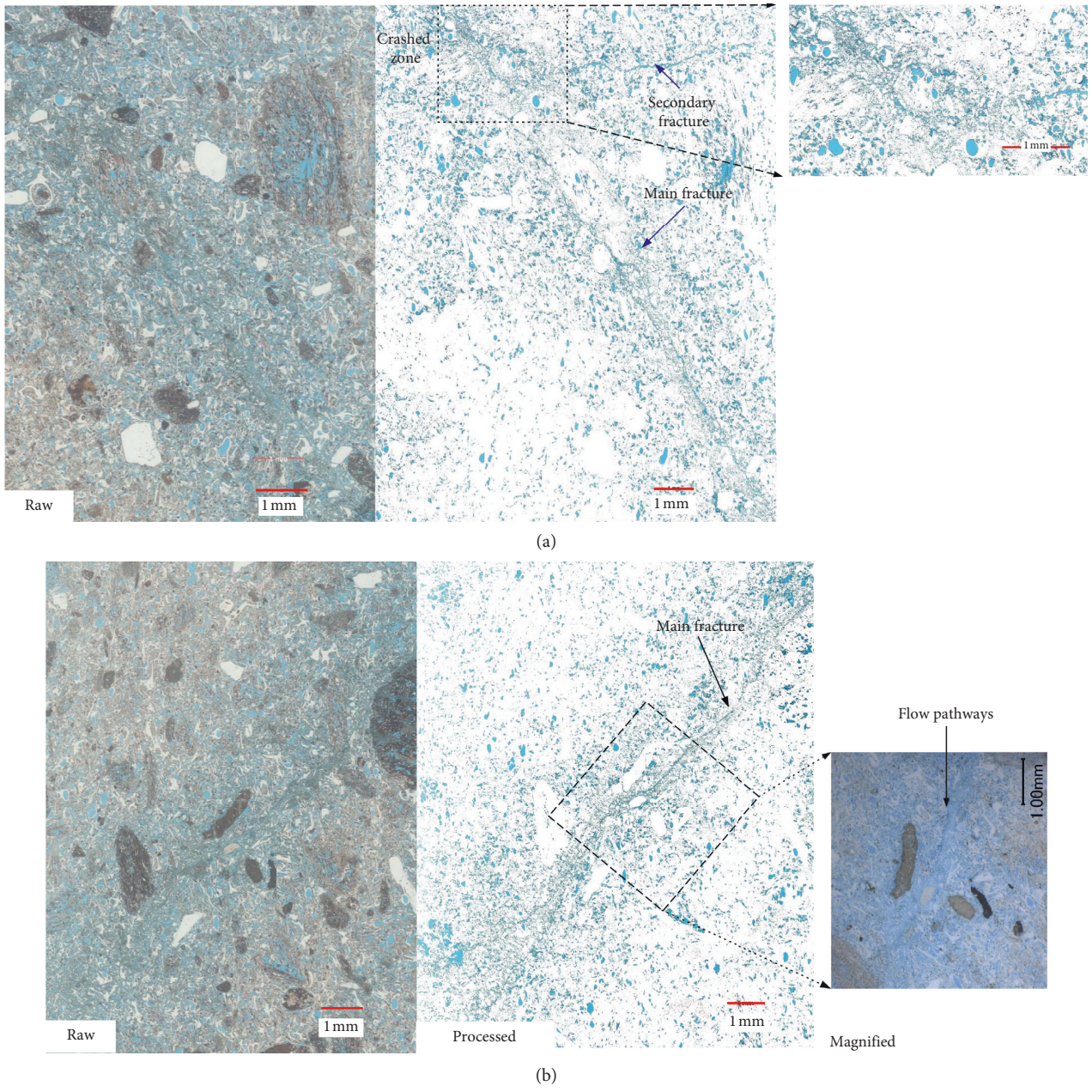

Figure 19: Images of blue resin impregnated thin-section samples after the tests under (a) $\Delta\sigma_A = 8$ MPa, $P_C = 5$ MPa, $P_P = 0.5$ MPa and (b) $\Delta P_P = 0.8$ MPa, $P_C = 5$ MPa, $P_P = 0.5$ MPa. Left: original images, middle: processed images to emphasize the blue resin, and right: magnified images.

4.2. Pore Pressure Disturbances. The pore pressure disturbances that were performed under 0.5 MPa in pore pressure (Figure 20) exhibited results that were similar to those of the axial stress disturbance.

The results under 0.1 MPa in pore pressure (Figure 21) were also similar to those of the axial stress disturbances. However, the effects of the disturbances were not clear because the amplitude of the pore pressure disturbances at 0.1 MPa in pore pressure was just 0.06 MPa. The results basically showed a good repeatability of the tests, except for the reduction of the permeability due to rock failure, which varied from specimen to specimen.

The k_2/k_1 ratio with zero disturbances was found to be less than one at 0.1 MPa in pore pressure and greater than one at 0.5 MPa in pore pressure (Figure 22(a)). This is the same result that was found for the axial stress disturbances and would indicate that, for the intact rocks, a higher pore pressure promoted a more rapid flow that cleaned up the trapped particles in the pore throats [10, 22–25]. Fractured rocks experienced a greater reduction in permeability under the lower

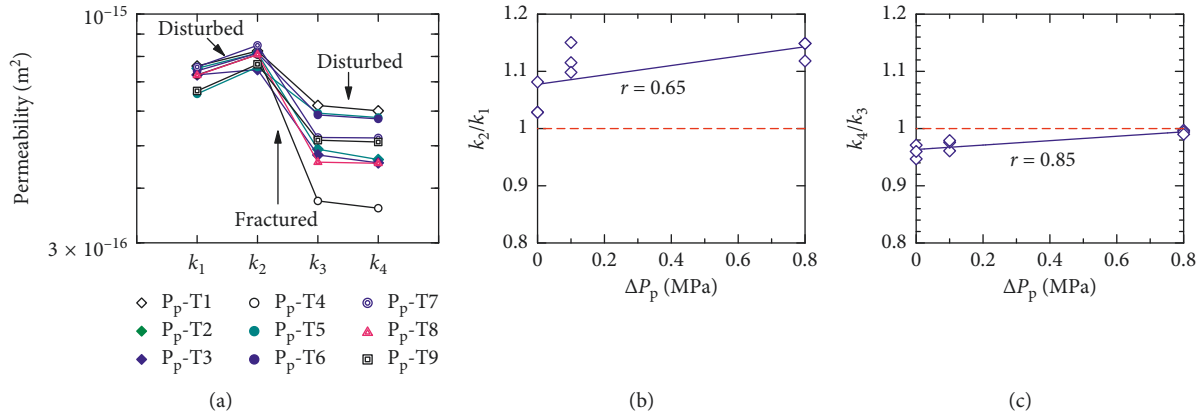

FIGURE 20: Variation in permeability (a), and permeability ratios of the intact rocks (b) or fractured rocks (c) ($P_P = 0.5$ MPa) due to transient pore pressure disturbances and triaxial compression of the Shikotsu welded tuff.

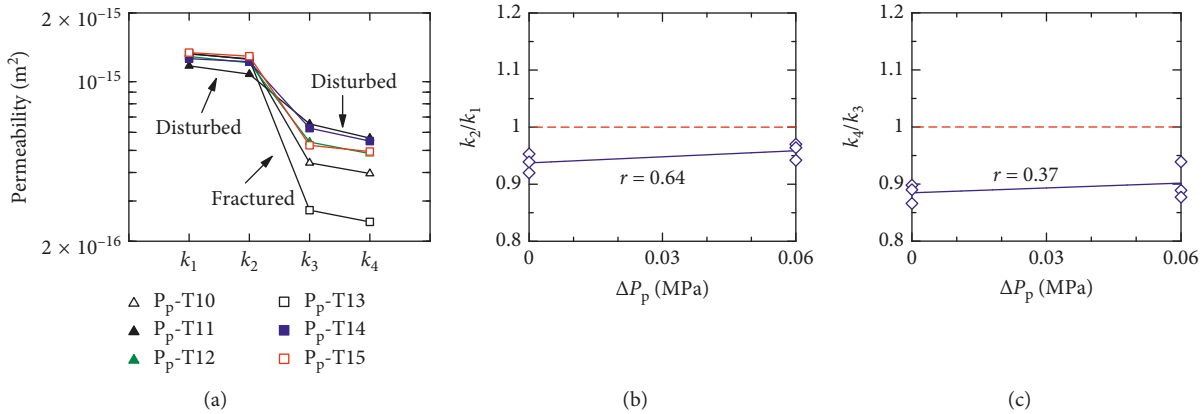

FIGURE 21: (a) Variation in permeability, and permeability ratios of the intact rocks (b) and the fractured rocks (c) due to transient pore pressure disturbances and triaxial compression of the Shikotsu welded tuff ($P_P = 0.1$ MPa).

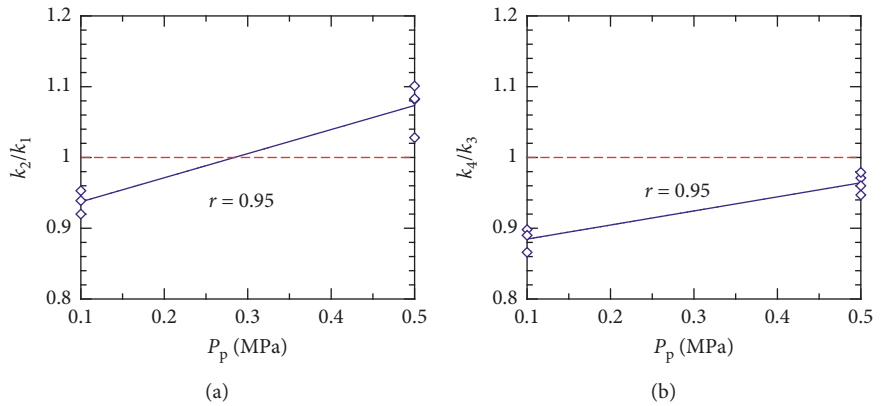

FIGURE 22: Effect of pore pressure on permeability ratios without stress disturbances. (a) Intact; (b) fractured.

pore pressure (Figure 22(b)), which may suggest that more particles were accumulated owing to the lower water flow.

5. Summary of the Results and Discussion

The effects of transient axial stress disturbances and pore pressure disturbances on the permeability values of Kushiro Cretaceous sandstone and Shikotsu welded tuff were investigated under various disturbance amplitudes. The results are summarized as follows.

The permeability of the Kushiro Cretaceous sandstone (Table 6) decreased at zero stress disturbances. For the intact rocks, the permeability reduction became larger as the confining pressure increased, but this was not exhibited by

Table 6: Summary of the variations in permeability of the Kushiro Cretaceous sandstone.

Disturbances	Intact	Fractured
Axial stress	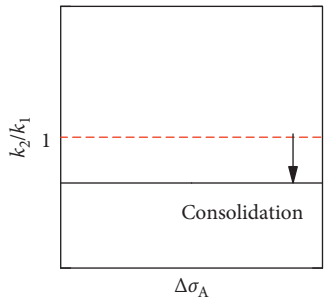	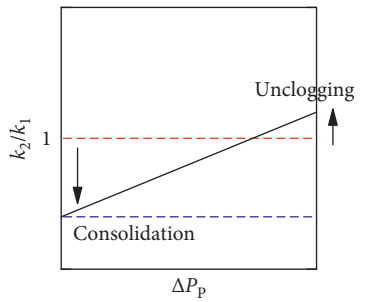
Pore pressure	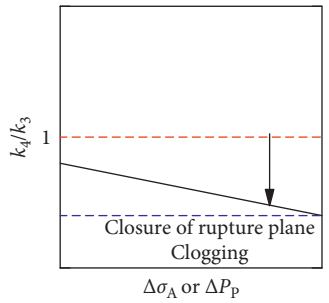	

the fractured rocks. In terms of the axial stress disturbance effects, the permeability was kept almost constant with the disturbance amplitude for the intact rocks. The reductions became larger as the disturbance amplitudes increased for the fractured rocks. Regarding the pore pressure disturbances, the reductions in permeability of the intact rocks decreased as the pore pressure disturbances increased, whereas the reductions increased as the disturbance amplitudes increased for the fractured rocks.

For the case of the Shikotsu welded tuff (Table 7), virtually the same results were obtained for both the axial stress and pore pressure disturbances. The permeability values of the intact rocks under 0.5 MPa in pore pressure increased at zero stress disturbances. They decreased under 0.1 MPa in pore pressure with no stress disturbances. The permeability (increase or decrease) was not affected by the disturbance amplitude. The permeability of the fractured rocks decreased at zero stress disturbances, and the reductions in permeability decreased as the disturbance amplitudes increased, and a permeability increase was even observed in some cases.

These results suggest that the permeability basically shows an initial decrease over time because the permeability measurements were not carried out after a sufficiently long time for the convergence of the consolidation. However, after the initial decrease, the stress disturbances would basically cause an increase in the permeability. If the rock contains a considerable amount of clay minerals, the increasing effect may be offset by a decrease in permeability due to enhanced consolidation caused by the stress disturbance. The consolidation effect was relatively stronger in the fractured rocks. This would happen because of the plastic and viscous deformations, along with the elastic deformations, of the mineral particles on and near the ruptured surface.

The increasing effect of the pore pressure disturbances was so strong that even the permeability of the intact Kushiro Cretaceous sandstone increased as the disturbance amplitude increased. This would occur because the pore pressure increases isotropically, enlarging the water flow path to remove particles, whereas the axial stress disturbances act only in the axial direction.

Considering that the effects of transient stress disturbances of rock masses would be different from those of intact rocks but not so significantly different from those of fractured rocks and considering that similar effects are likely to occur for similar rock types, it is expected that the permeability of rock mass consisting of argillaceous/glassy rocks may decrease/increase owing to transient stress disturbances.

6. Concluding Remarks

To clarify the effects of transient stress disturbances on the rock permeability, permeability measurements were carried out on intact and triaxially fractured Kushiro Cretaceous sandstone and Shikotsu welded tuff before and after axial stress or pore pressure transient disturbances. According to the experimental results, the stress disturbances showed either decreasing or increasing effects on the permeability depending on the rock type and experimental conditions.

The permeability of the Kushiro Cretaceous sandstone decreased at zero stress disturbances. For the intact rocks,

Table 7: Summary of the variations in permeability of the Shikotsu welded tuff.

Disturbances	Intact	Fractured
Axial stress	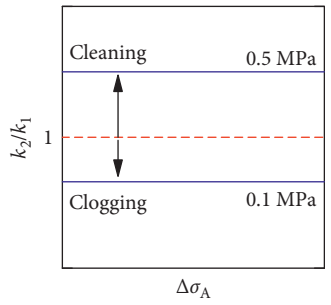	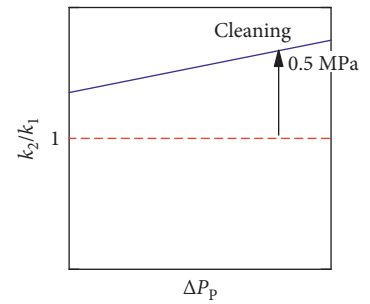
Pore pressure	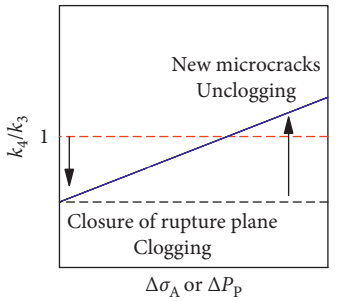	

the permeability was kept almost constant with the disturbance amplitude. For the fractured rocks, the reductions became larger as the disturbance amplitudes increased. Regarding the pore pressure disturbances, the reductions in permeability of the intact rocks decreased as the pore pressure disturbances increased, whereas the reductions increased as the disturbance amplitudes increased for the fractured rocks.

For the Shikotsu welded tuff, virtually the same results were obtained for both the axial stress and pore pressure disturbances. There were negligible effects of stress disturbances for the intact rocks. The permeability of the fractured rocks decreased at zero stress disturbances, and the reductions in permeability decreased as the disturbance amplitudes increased, and a permeability increase was even observed in some cases.

When focusing on the fractured rocks rather than the intact rocks, which would be more important in field applications, the argillaceous Kushiro Cretaceous sandstone mainly exhibited decreasing effects. In contrast, the glassy Shikotsu welded tuff mainly exhibited increasing effects.

The permeability variations due to transient stress disturbances have already been used as a seismic wave-enhanced oil recovery (EOR) technique, in which an increase in permeability due to the movement of the entrapped fluid in the reservoir [6] is expected. An increase in the permeability may encourage its future utilization to enhance natural gas recovery, to prevent large earthquakes by inducing a large number of small earthquakes [4, 8, 17], and to reroute an underground water flow for various purposes. A decrease in the permeability could be used in the future to help seal rock caverns and to reroute an underground water flow for various purposes.

Further experiments on different rock types under various conditions along with investigations of the mechanisms of the variations in permeability will assist the clarification of the effects of transient stress disturbances. The persistency of the variations in permeability, among other aspects, should also be investigated in the future.

Data Availability

The data used in this study are available from the corresponding author upon request.

Conflicts of Interest

The authors declare that there are no conflicts of interest regarding the publication of this paper.

Acknowledgments

This research was supported by the Japan International Corporation Agency (JICA) under the AUN/SEED-Net program (J16-10145).

References

[1] C. Wang and Y. Chia, "Mechanism of water level changes during earthquakes: near field versus intermediate field," *Geophysical Research Letters*, vol. 35, no. 12, 2008.

[2] Y. Orihara, M. Kamogawa, and T. Nagao, "Preseismic changes of the level and temperature of confined groundwater related

to the 2011 Tohoku earthquake," *Scientific Reports*, vol. 4, no. 1, p. 6907, 2014.

[3] Y. Fujii, Y. Ichihara, H. Matsumoto, J. Kodama, D. Fukuda, and A. B. Dassanayake, "Water drainage from Kushiro coal mine decreased on the day of all $M \geq 7.5$ earthquakes and increased thereafter," *Scientific Reports*, vol. 8, article 16472, 2018.

[4] M. Manga, I. Beresnev, E. E. Brodsky et al., "Changes in permeability caused by transient stresses: field observations, experiments, and mechanisms," *Reviews of Geophysics*, vol. 50, 2012.

[5] M. Manga and C. Wang, "4.12. Earthquake hydrology," *Treatise on Geophysics*pp. 305–328, Elsevier, Oxford, UK, 2nd edition, 2015.

[6] S. R. Pride, E. G. Flekkøy, and O. Aursjø, "Seismic stimulation for enhanced oil recovery," *Geophysics*, vol. 73, no. 5, pp. O23–O35, 2008.

[7] I. A. Beresnev, R. D. Vigil, W. Li et al., "Elastic waves push organic fluids from reservoir rock," *Geophysical Research Letters*, vol. 32, no. 13, 2005.

[8] Y. Fujii, M. Sheshpari, J.-i. Kodama, D. Fukuda, and A. Dassanayake, "Prevention of catastrophic volcanic eruptions, large earthquakes underneath big cities, and giant earthquakes at subduction zones," *Sustainability*, vol. 10, no. 6, p. 1908, 2018.

[9] J. E. Elkhoury, A. Niemeijer, E. E. Brodsky, and C. Marone, "Laboratory observations of permeability enhancement by fluid pressure oscillation of in situ fractured rock," *Journal of Geophysical Research: Solid Earth*, vol. 116, no. B2, 2011.

[10] P. M. Roberts, "Laboratory observations of altered porous fluid flow behavior in Berea sandstone induced by low-frequency dynamic stress stimulation," *Acoustical Physics*, vol. 51, no. S1, pp. S140–S148, 2005.

[11] V. M. Shmonov, V. M. Vitovtova, and A. V. Zharikov, "Experimental study of seismic oscillation effect on rock permeability under high temperature and pressure," *International Journal of Rock Mechanics and Mining Sciences*, vol. 36, no. 3, pp. 405–412, 1999.

[12] W. Liu and M. Manga, "Changes in permeability caused by dynamic stresses in fractured sandstone," *Geophysical Research Letters*, vol. 36, no. 20, 2009.

[13] Y. Fujii, Y. Ishijima, Y. Ichihara et al., "Mechanical properties of abandoned and closed roadways in the Kushiro Coal Mine, Japan," *International Journal of Rock Mechanics and Mining Sciences*, vol. 48, no. 4, pp. 585–596, 2011.

[14] S. Doi, "Petrological and petrochemical studies of welded tuff," *Reports of the Geological Survey of Japan*, vol. 29, pp. 30–103, 1963.

[15] A. Alam, Y. Fujii, D. Fukuda, and M. Niioka, "Temperature-confining pressure coupling effects on the permeability of three rock types under triaxial compression," *Rock Engineering and Rock Mechanics: Structures in and on Rock Masses*, pp. 131–136, 2014.

[16] J. Bear, *Hydraulics of Groundwater McGraw-Hill Series in Water Resources and Environmental Engineering*, vol. 463, McGraw-Hill, New York, NY, USA, 1979.

[17] C. Wang and M. Manga, *Earthquakes and Water*, Springer, Berlin, Germany, 2009.

[18] J. E. Elkhoury, E. E. Brodsky, and D. C. Agnew, "Seismic waves increase permeability," *Nature*, vol. 441, no. 7097, pp. 1135–1138, 2006.

[19] I. Beresnev, W. Gaul, and R. D. Vigil, "Direct pore-level observation of permeability increase in two-phase flow by shaking," *Geophysical Research Letters*, vol. 38, 2011.

[20] R. Bai and C. Tien, "Particle detachment in deep bed filtration," *Journal of Colloid and Interface Science*, vol. 186, no. 2, pp. 307–317, 1997.

[21] J. Bergendahl and D. Grasso, "Prediction of colloid detachment in a model porous media: hydrodynamics," *Chemical Engineering Science*, vol. 55, no. 9, pp. 1523–1532, 2000.

[22] J. E. Elkhoury, A. Niemeijer, E. E. Brodsky, and C. Marone, "Dynamic stress stimulates flow in fractures: laboratory observations of permeability enhancement," *Journal of Geophysical Research*, vol. 115, 2010.

[23] E. E. Brodsky, E. Roeloffs, D. Woodcock, I. Gall, and M. Manga, "A mechanism for sustained groundwater pressure changes induced by distant earthquakes," *Journal of Geophysical Research: Solid Earth*, vol. 108, no. B8, 2003.

[24] T. Candela, E. E. Brodsky, C. Marone, and D. Elsworth, "Laboratory evidence for particle mobilization as a mechanism for permeability enhancement via dynamic stressing," *Earth and Planetary Science Letters*, vol. 392, pp. 279–291, 2014.

[25] T. Candela, E. E. Brodsky, C. Marone, and D. Elsworth, "Flow rate dictates permeability enhancement during fluid pressure oscillations in laboratory experiments," *Journal of Geophysical Research: Solid Earth*, vol. 120, no. 4, pp. 2037–2055, 2015.